

Hydrologic and Geochemical Controls on St. Louis River Chemistry with Implications for Regulating Sulfate to Control Methylmercury Concentrations



11/3/2014

Michael Berndt¹, Jeff Jeremiason², and Benjamin Von Korff³

¹Minnesota Department of Natural Resources
500 Lafayette Rd
St. Paul, MN 55455

²Gustavus Adolphus College
Department of Chemistry
800 West College Avenue
St. Peter, Minnesota, 56082

³Mankato State University
Water Resources Center
184 Trafton Science Center South
Mankato, MN 56001

Abstract

Water discharged from taconite mines currently provides the majority of sulfate (SO₄) to the St. Louis River in NE MN. This report represents one of a series of linked studies conducted in 2012 in the St. Louis River watershed detailing impacts of SO₄ from mining on mercury cycling in areas downstream from the mining region. Here, focus is placed on SO₄, magnesium (Mg), dissolved organic carbon (DOC), total mercury (THg), MeHg, and iron (Fe) concentrations from 33 samples collected systematically from three sites on the St. Louis River from May to October in 2012. Two of the sampling sites were located immediately upstream (Mile 179) and downstream (Mile 94) from the mining region and a third was located well downstream (Mile 36) following dilution by waters from several large tributaries not impacted by mining.

Principal component analysis reveals strongly independent behavior for mining (Mg and SO₄) and non-mining (DOC, THg, MeHg, and Fe) components. Mg and SO₄ concentrations in the samples developed two strong parallel mixing trends ($r^2=0.99$) owing to the dilution and mixing of relatively small amounts of mine water containing high Mg and SO₄ with generally much larger and variable volumes of water from non-mining portions of the watershed containing lesser amounts of these elements. The mixing trends imply that the relative amounts of Mg and SO₄ delivered from mines remained fixed throughout the period while those derived from the rest of the watershed shifted. The strong linearity of the trends implies that SO₄ from the mines behaved relatively conservatively during transport since its reduction to sulfide would generate a decrease in SO₄ but not Mg. This contrasts to SO₄ concentrations upstream from the mining region, which declined from about 4 mg/l in May to less than 1 mg/l in August.

THg, MeHg, and Fe all increased with DOC similarly among the three sites during the wet portion of the season, but diverged somewhat as conditions dried out for the remainder of the summer as the DOC transported in streams was accompanied by high Fe and less THg. MeHg concentrations remained similar among sites despite considerably higher DOC concentrations at the upstream site compared to the downstream sites. The data are consistent with the mixing of waters derived from base flow (mines and groundwater) with an interlayer component containing elevated DOC, Fe, THg, and MeHg. The deepening of flow paths that accompany reduced flow rate into the rivers is accompanied by depletion of SO₄ and increased Mg and Fe concentrations. MeHg appears to be generated throughout the watershed when waters containing SO₄ above about 1 mg/L are forced through riparian soils and wetland sediments into nearby surface waters. This model implies that constraining SO₄ levels in water pumped into the headwater regions directly from mines would have little impact on MeHg concentration in the St. Louis River since the vast majority of MeHg in the St. Louis River is generated in areas not impacted by SO₄ from the mining region.

Table of Contents

Contents

Abstract	2
Table of Contents	3
Introduction	4
Sample site selection	5
Chemical methods	5
Field sampling and measurements	5
Major Cations and Anions.....	6
Dissolved Organic Carbon (DOC)	7
THg and MeHg	7
Results.....	7
St. Louis River Flow measurements during 2012.....	7
Concentrations.....	8
Discussion.....	9
Summary and Implications	14
Acknowledgements.....	15
Figures.....	16
Tables	24
Appendix - Data Tables	27
References	30

Introduction

The upper St. Louis River watershed in NE Minnesota hosts a large iron ore mining district that has operated continuously since the 1890s. The district, which contains many open pit mines and small to medium sized mining communities, is located in the northern headwater regions of a watershed dominated by forests, wetlands, and limited agricultural production (Figure 1). It has long been known that mining activities on the Iron Range result in release of SO_4 to the St. Louis River (Berndt and Bavin, 2009; Maderak, 1963; Moyle and Kenyon, 1947). Most of this SO_4 is released by the oxidative dissolution of minor iron sulfide minerals in stockpiles and tailings placed above water level in pits or directly on the land. In 2010 and 2011, the mining region contributed an estimated average of 35 metric tons/day of SO_4 to the St. Louis River (Berndt and Bavin, 2012a) which compares to approximately 15 metric tons/day from non-mining portions of the watershed.

The St. Louis River and its estuary are considered impaired with respect to the MeHg concentration in fish tissue (MPCA, 2013). Once it enters the food chain, MeHg persists and accumulates progressively up the food chain, potentially producing toxic effects to species at higher trophic levels (loons, eagles, sport fish, fish-consuming humans). SO_4 reducing bacteria (SRB) can participate in both mercury methylating (Benoit et al., 1999; Gilmour et al., 1992) and demethylating (Marvin-Dipasquale et al., 2000) reactions, and, thus, it is important to determine if and how SO_4 from mining impacts mercury geochemical cycles in this river.

The Minnesota Department of Natural Resources began studying relationships between SO_4 and MeHg in the St. Louis River and its watershed in 2007 (Berndt and Bavin, 2009, 2011, 2012a,b). Little difference could be found between MeHg concentrations in mining and non-mining tributaries and the river's chemistry appeared to be made up of a relatively conservative mixture of inputs from mining and non-mining streams. Except in special instances the geochemical relationships between MeHg, THg, and DOC examined throughout the St. Louis River watershed were found to be similar to those reported previously for a well-studied nearby watershed that lacked any high SO_4 inputs (Balogh et al., 2004; Balogh et al., 2006).

These previous studies were all conducted under conditions of moderate to low flow, when mercury and methylmercury concentrations are also typically low in streams (Brigham et al., 2009). The present study provides data and interpretation for 33 new samples collected systematically from the St. Louis River between May and October 2012, a period characterized by historically high rainfall and river volumes in June and a long dry period that lasted through October. Thus, data from the present study can be used to provide insights on the major processes affecting the sulfur and Hg cycling in the St. Louis River for the full range of flow conditions likely to be encountered in this region. Moreover, other studies conducted during

this same time period evaluated MeHg and THg concentrations in dragonfly larvae (Jeremiason et al., 2014a), methylation and sulfur dynamics in lakes and lake sediments exposed to elevated SO₄ (Bailey et al., 2014 a,b), MeHg binding to DOC (Jeremiason et al., 2014b), photodemethylation (Jeremiason et al., 2014c), and sulfur and oxygen isotope ratios for dissolved SO₄ in streams and waters throughout the watershed (Kelly and Berndt, 2014). The present study provides a “big picture” look at element distributions and mining impacts for samples collected upstream and downstream from the mining region in the St. Louis River, while the other studies provide more focused examination of specific geochemical processes that take place in high-SO₄ impacted areas located primarily in the mining region.

Sample site selection

Three sampling sites in the St. Louis River were chosen to maximize the ability to evaluate mixing and reactivity of waters derived from mining and non-mining portions of the St. Louis River watershed (Figure 1, Table 1). The three sampling sites are named according to approximate distance (miles) from the St. Louis River’s estuary. The site at Mile 179 is located just upstream from the first possible impact from mining tributaries. The site at Mile 94 is located just downstream from the Swan River, the last tributary that carries any mining water into the St. Louis River. The site at Mile 36 is located well downstream from the mining region, following inputs from a number of small and large non-mining tributaries (Whiteface, Cloquet, and Floodwood) and just before the water flows through a series of dams and, eventually to its estuary in Lake Superior. Sampling at each of the three sites was conducted on a two to three week cycle, beginning in May and ending in late October in 2012 (See Figure 2).

Discharge volumes were monitored continuously throughout the study at three sites along the river. The first is referred to as the “Skibo” site in this study, which is the same as our Mile 179 sampling site. The second is in Forbes, MN, which is located near the center of the mining district, between the Mile 94 and Mile 179 sampling sites. The final location is the “Scanlon” site which is near Cloquet, located approximately three miles downstream from the Mile 36 sampling site.

Chemical methods

Field sampling and measurements

Water samples were collected using a peristaltic pump connected to Teflon tubing that was extended out into the stream along a 24 ft sampling pole configured with a plastic float. The end of the tubing was directed downward from the float so that samples were collected from 6 and 12 inches below the surface. The tubing, filtration apparatus, and sample bottles were all

conditioned thoroughly by pumping at least 300 mls of river water from the site prior to drawing any samples used for analysis.

Water quality parameters (Salinity, Temperature, Specific Conductivity, pH, ORP, DO) were measured using a YSI 556 MPS sonde from Yellow Spring Instruments. Three probes were attached to the sonde: pH/ORP (YSI 5565), temperature/conductivity (YSI 5560), and dissolved oxygen (Sensor - YSI 559, Membrane cap, 2ml – YSI 5909). Probes were calibrated daily, and the calibration was checked half-way through the field day.

DOC samples were collected and stored in 40ml amber non-processed vials while alkalinity, cation, and anion samples, were stored in 60ml HDPE bottles. The cation samples were preserved in the field by adding 200 µl ultra-pure nitric acid. Unfiltered samples collected for nutrient analyses were stored in 500 ml Nalgene bottles, and preserved at the Hibbing lab with 1 ml 93-98% H₂SO₄.

THg and MeHg samples were collected using clean hands-dirty hands techniques. Samples were filtered through ashed (550 C), 47mm glass fiber filters (0.7 micron nominal pore size) and stored on ice and in the dark in double-bagged 125ml PETG bottles. THg and MeHg samples were preserved with 12 M HCl (0.5% by volume). Duplicate and procedural blanks for all samples were collected approximately every 10 samples.

Major Cations and Anions

Cation and anion samples were shipped overnight and on ice to the University of Minnesota Analytical Geochemistry Lab, Minneapolis, Minnesota. Cations were analyzed on a Thermo Scientific iCAP 6500 duo optical emission spectrometer (serial no. 20083410) fitted with a simultaneous charge induction detector. The system has separate slit openings for the low wavelengths < 232 nm and for those greater. All elements were measured on the most appropriate wavelength that is determined by the estimated composition, need for sensitivity, and the avoidance of element spectral overlaps. For each sample, standard, and blank the data is replicated 5 times to determine a mean and standard deviation for each selected elemental wavelength. Calibration is accomplished by comparing a NIST traceable single or multi-element standard solution to the unknowns. All blanks, standards, and samples are acid matrix matched to lessen matrix effects and are diluted such that element concentrations are in the linear working range of the standard and detector combination.

Anions were analyzed on a Dionex ICS-2000 ion chromatography system consisting of an AS11 analytical column, AMMS III suppressor, AS40 autosampler, and integrated dual piston pump and conductivity detector. The eluent is generated by Dionex's patented Reagent Free eluent generator system, which produces a variable concentration KOH eluent depending upon the request of the computer based software.

Dissolved Organic Carbon (DOC)

All dissolved organic carbon samples were shipped overnight and on ice to the United States Geological Survey in Boulder Colorado where they were analyzed in the lab of Dr. George Aiken. DOC was determined by a wet oxidation method using an OI analytical Model 700 TOC Analyzer. UV-Vis spectra were measured in a 1-cm path length quartz cell using a Hewlett-Packard Photodiode Array Spectrophotometer (model 8453). Absorption at 254 nm (UV_{254}) was corrected for iron content and used to determine SUVA which is the UV_{254} absorbance (m^{-1}) divided by DOC concentration (mg/L) (Burns et al., 2013).

THg and MeHg

All of the preserved THg and MeHg samples were shipped within a few days of sampling, overnight and on ice, to Gustavus Adolphus College in St. Peter, Minnesota where they were further processed and analyzed.

Filtered Total Mercury (THg) concentrations were determined by standard stannous chloride reduction dual-amalgamation techniques using accepted trace-metal clean techniques (Fitzgerald and Gill, 1979). Acidified samples from the field collections were transferred to 50 mL autosampler vials and oxidized with bromine monochloride for at least 12 hours then neutralized with hydroxylamine hydrochloride. Stannous chloride was added prior to Hg analysis on a Brooks Rand MERX automated mercury analyzer equipped with a total Hg module and a Brooks Rand Model III Atomic fluorescence spectrophotometer.

Methylmercury (MeHg) concentrations were measured using standard ethylation/isotope dilution techniques. Acidified samples from field collections were spiked with a known amount of isotopically enriched MeHg ($Me^{201}Hg$). Following a sub-boiling distillation, distillate pH was adjusted to ~4.8 with a sodium acetate buffer and MeHg species were ethylated using sodium tetraethyl borate. Following ethylation, samples were analyzed on an Agilent 7700 ICP-MS (inductively coupled plasma – mass spectrometer) connected to a Brooks Rand MERX system using an isotope dilution method (Hintelmann and Evans, 1997).

Results

St. Louis River Flow measurements during 2012

The three gaging stations all registered similar flow patterns throughout the sampling season (Figure 2), indicating that the main rainfall events impacted the whole region in similar fashion throughout the summer. The most upstream site, at Skibo (Mile 179), registered a maximum flow that reached close to 800 cfs in late June, but this fell to only 1 cfs in early October. At

Forbes, in the middle of the mining region, maximum and minimum flow rates were approximately 5000 and 40 cfs, respectively, while flows at Scanlon ranged from approximately 40000 down to 400 cfs. The 40,000 cfs measured at Scanlon in late June was an all-time high flow record for the station and produced historic flooding in Duluth, downstream. Table 2 contains estimated flow rates for the Mile 94 sampling site. These were computed by multiplying the measured flows at Forbes by 1.746, a correction factor calculated by dividing the watershed area upstream from Mile 94 (1208 sq miles) by that upstream from Forbes (692 sq miles). Estimated flow rates at this site on sampling dates ranged from 82 to 6313 cfs (Table 2).

Sampling was conducted systematically throughout the season (Figure 2) and so represented both very high and very low flow conditions. Each of the first three samples at each site was collected under higher flow conditions than the preceding sample, but, thereafter, the flow levels progressively declined throughout the summer months in response to an extremely dry period.

All mine water discharges are monitored and reported on an annual basis to the Minnesota Department of Natural Resources. For comparison purposes, recent discharge from taconite mines to the St. Louis River averaged approximately 70 CFS (DNR records) which is slightly lower than the minimum estimated flow rate estimated at our Mile 94 sampling site. Discharge from mines consists mostly of groundwater and occurs at a comparatively fixed rate throughout the year. However, pumping rates can be increased or decreased to accommodate wet or dry conditions, or when dewatering rates need to be modified for other reasons. The 70 CFS average value is close to the entire estimated flow volume for the river at Mile 94 in September and October when conditions were dry, but ranges between 11 and 17% of the flow at this site that was recorded between late May and early August. Thus, stream flow at site 94 was dominated by non-mining waters early in the year, but transitioned to domination by input of mine water late in the year. The 70 CFS mine water average flow rate represents only 0.3 to 16% of the flow volume measured at Scanlon for the wettest and driest conditions, respectively. This site, therefore, always contains a mixture of mining and non-mining inputs but is dominated by non-mining inputs throughout the year and especially during wet periods.

Concentrations

This study focuses on a comparison of the behaviors of components typically found in mine waters (Mg and SO₄) with those thought to be derived mostly from the non-mining region (DOC, THg, MeHg, Fe) (Tables 2a to 2c) (Berndt and Bavin, 2012a). Full chemistry for waters collected at each of these sites in 2012 is provided in the appendix.

The highest SO₄ and Mg concentrations (134 and 53.2 mg/L, respectively), indicative of the greatest percentage of mine inputs, were observed under dry conditions from the same sample collected near the end of the study at Mile 94, just downstream from the mining region. The

lowest concentrations for SO₄ were slightly below 1 mg/L for samples collected from Mile 179 site, upstream from the mining region as flow was subsiding in August. The lowest Mg concentration was a value of 3.1 mg/l for a sample collected from the Mile 179, upstream from the mining region when flow was at its peak in late June. SO₄ concentrations tracked Mg closely at Miles 94 and Mile 36, with concentrations of both decreasing during the high flow periods and then increasing through the rest of the summer as the area dried out. This is in distinct contrast to the relative behavior of these components at Mile 179 upstream from the region, where SO₄ concentrations distinctly decreased as Mg increased through July and early August.

DOC, MeHg, and THg concentrations behaved very similarly to each other in all of the watersheds, increasing in the first part of the study and then decreasing through the late summer and early fall. MeHg peaked relatively sharply at all sites in July when flow rates were still relatively high, but the highest concentrations occurred clearly after the highest flow rates were observed. THg peaked broadly at all sites from June through mid-July, but remained elevated at Mile 179 even after MeHg declined. DOC peaks occurred in mid-July at the Mile 33 and Mile 94 sites, but was delayed until August for the Mile 179 site, right when SO₄ concentrations reached minimum values. DOC, THg, and MeHg concentrations at Site 179 were almost always elevated compared to concentrations measured simultaneously at the other two sites. The one exception was a measured MeHg concentration of 1.14 ng/L from July 16 at the Mile 94 Site which is slightly elevated compared to the 1.10 ng/L measured for the Mile 179 Site on July 17.

Fe, an element typically found in reduced groundwater and soil environments, but which is nearly absent from mine waters (which are oxidizing and have high pH in this region), became especially elevated at all sites during the earliest part of the summer dry period, when flows were still relatively high but still declining relatively rapidly. Maximum concentrations were found at Mile 179 from mid-July to late August, clearly after the peak flow period in late June, but also when MeHg concentrations were declining. The maximum observed concentrations at Mile 94 and 33 were 2.6 mg/L and 2.18 mg/L, respectively, both in mid-July, but Fe concentrations quickly fell after that.

Discussion

A principal component analysis for concentrations of typical mining (Mg, SO₄) and non-mining (Fe, DOC, MeHg, and THg) chemicals were generally unrelated to each other (Figure 3). The clustering shows that Mg and SO₄ were very closely tied to each other but had almost no correlation to MeHg, and only a slight inverse relationship to THg, Fe, and DOC. Thus, while

other studies have demonstrated that the addition of SO₄ produces an increase in mercury methylation in peatlands (Åkerblom et al., 2013; Bergman et al., 2012; Coleman Wasik et al., 2012; Jeremiason et al., 2006), SO₄ concentration appears, for the most part, unrelated to MeHg concentration in the St. Louis River. Other studies have identified instances where methylation rates are inversely related to the SO₄ at relatively high concentrations in the range of those measured downstream from the mining region (Gilmour et al., 1998). Proposed mechanisms for an inverse relationship between SO₄ and MeHg production include formation of charged sulfide complexes and the formation of HgS nanocolloidal and aggregated particulates (Benoit et al., 1999; Gerbig et al., 2011) that make oxidized Hg unavailable for methylation. However, MeHg concentrations in the present study are not either positively or negatively correlated to total SO₄ concentrations measured in the streams.

We suggest that no correlation between MeHg and SO₄ in this river is primarily because the majority of SO₄ from mining is added directly to the headwaters with little or no opportunity, subsequently, to react with organic rich sediments in a manner needed to produce MeHg and transport it into the streams. Instead, MeHg is derived from the watershed as a consequence of recharge from precipitation throughout the watershed. Precipitation drives water containing SO₄ deposited with rainfall or weathered from soils through riparian and wetland sediments containing labile organic carbon and mercury and into surface waters throughout the watershed, conditions ideal for generating streams rich in MeHg (Vidon et al., 2010). Below, we use chemical relationships from the present data set to show that MeHg concentrations became elevated throughout the watershed precisely when SO₄ from non-mining areas was reduced from several mg/L down to less than 1 mg/L and also when Fe and DOC became enriched suggesting reactions occurred in organic rich-sediments containing relatively low sulfide.

Mg and SO₄ correlation: Mg and SO₄ concentrations in the St. Louis River remained remarkably correlated ($r^2=0.982$) in 2012 despite the extreme variability in hydrologic conditions. Partitioning the data into “wet” (May and June) and “dry” (July to October) periods (Figure 4) reveal two distinct but generally parallel trends with even stronger correlations ($r^2=0.989$ for wet and 0.991 for dry period). The strong linearity of the two trends imply (1) that Mg and SO₄ from mines were added throughout the summer months in direct proportion to each other and (2) that the Mg:SO₄ ratio of the mining component (e.g., slope of the line) was not changed significantly by chemical processes taking place in the river or its tributaries. The former reflects the fact that mining is a continuous process and that the averaged blended output from mine-dewatering processes changed relatively little throughout the year. The latter implies that the net loss of sulfate to sulfide reduction within the watershed (Bailey et al., 2014 a, b; Berndt and Bavin, 2011) is small compared to the mass of SO₄ transported in the river.

The strong linearity but change in intercept of each trend implies that average Mg levels increased during the dry period both upstream and downstream from where the high Mg and SO₄ waters were pumped from the mines. This type of relationship, is directly verified for Mile 179 (Figure 5), but can only be inferred from the mixing trends for the remainder of the watershed. At Mile 179, the SO₄ concentration fell from near 4 mg/L to just under 1 mg/L as Mg peaked suggesting that unlike the mining component, there is a substantial loss in SO₄ relative to Mg for background waters. SO₄ reduction and Mg increases have been shown to accompany reduced recharge to streams in riparian zones elsewhere (Bishop et al., 2004; Köhler et al., 2009; Vidon et al., 2010), an effect attributed to greater degrees of reaction between the waters feeding the streams and minerals encountered along deeper flow-paths.

Importantly, it has been found that while Mg and SO₄ concentrations deviate narrowly from the mixing relationships in Figure 4, O-isotopic ratios for dissolved SO₄ in the St. Louis River at Mile 36 is highly elevated compared that expected for a simple mixture of SO₄ derived from mines and SO₄ derived from other background sources (Berndt and Bavin, 2012a; Kelly and Berndt, 2014). This implies that SO₄ added from mines is not entirely non-reactive during transport through the watershed. A precise isotope exchange mechanism has not been identified, but may involve partial and reversible reduction of SO₄ in hyporheic zones or in the stratified lakes encountered by mining tributaries.

THg, MeHg, and Fe vs DOC: In contrast to Mg and SO₄, mine waters typically have very little Hg, DOC, or Fe (Berndt and Bavin, 2011) and so the great majority of these components in the St. Louis River must be introduced into streams during recharge from non-mining portions of the watersheds. MeHg, THg, and Fe were obviously correlated with DOC in the present study, but these correlations changed somewhat as watershed conditions shifted from wet to dry and also among the three sites (Figure 6). Analyzing the similarities and differences among sites can provide useful insights into important production and transport processes for MeHg.

THg, MeHg, and Fe versus DOC relationships during the wet period, for example, were quite similar for samples collected from all of the sites, whether located upstream or downstream from the mining region (dashed patterns in Figure 5). This suggests strongly, that similar production and transport mechanisms governed the concentrations for these components throughout the region during high-flow conditions. THg:DOC ratio decreased at all three sites when conditions transitioned from wet (dashed) to dry (solid patterns in Figure 6) and then both DOC and THg decreased together. This created a clockwise rotation in the THg vs DOC plots for all three sites. This is in contrast to MeHg:DOC relationships which revealed a clockwise rotational pattern at Mile 179, but not at the other sites, where MeHg and DOC concentrations during the dry period effectively retraced the same linear relationship observed during the wet period. The trends suggest that the water upstream from the mining region

contained an extra DOC component with lower Hg and MeHg than the DOC found at the downstream sites.

Berndt and Bavin (2012b) found that mining tributaries generally carried lower DOC concentrations than non-mining streams sampled throughout the watershed despite having similar MeHg concentrations to each other when sampled under similar flow conditions. They used this observation and differences in filterability of waters to suggest that a fraction of the DOC containing little or no MeHg was flocculating out when elevated Mg and SO₄ were encountered in mining tributaries. This mechanism could potentially account for the observed trends, but has not been demonstrated in a laboratory and so must still be considered a preliminary interpretation.

The present samples were also analyzed for their absorbance at wave length 254 nm and results were corrected for Fe and divided by and translated to SUVA (Wave length 254, SUVA, corrected for Fe (Figure 7). High SUVA values for the more dilute waters at Mile 179 represent the presence of highly aromatic carbon in the DOC, while the low SUVA values in high sulfate waters reveal this fraction is missing. If it is assumed that DOC sources were similar in the source regions, then it is possible that the addition of Mg and SO₄ from mines caused partial loss of the high SUVA fraction. On the other hand, the present study did not determine whether other factors relating to geography and wetland percentages can explain the differences in DOC concentration and quality at site 179 compared to the downstream sites. Moreover, the most elevated SO₄ concentrations represent flow under dry conditions when residence time and potential for in-stream degradation of DOC (either in the water column or in hyporheic zones) is higher. The reason for the change in quality and quantity of DOC remains unknown.

In contrast to the clockwise rotation suggested by THg vs DOC plots, the Fe:DOC ratio increased at all three sites when conditions transitioned from wet to dry and produced a *counterclockwise* rotation in Fe versus DOC plots. The abrupt Fe increase at Mile 179 occurred just as SO₄ concentrations dipped below 1 mg/L (See Table 2, Figure 5), a value thought to be needed for SO₄ reduction to occur (Corrales et al., 2011). Loss of available SO₄ has also been used by Knorr (2013) to link increases in both Fe and DOC in drainage from catchments throughout Europe and North America. Once SO₄ is consumed, then the DOC is produced under conditions of Fe reduction. The Fe versus DOC trends in the present study were strikingly parallel, indicative of the DOC having been produced under Fe-reducing conditions throughout the watershed during the dry period. This would imply that that SO₄ was similarly depleted in the recharge zones throughout the watershed during this time period.

Recharge to streams: Recharge to watersheds following a precipitation event is a complex process involving a number of hydrologic and geochemical processes that act together to

control the chemistry of waters that run off the land into streams (Bishop et al., 2004; Grabs et al., 2012; Köhler et al., 2009; Lyon et al., 2011; Seibert et al., 2009; Vidon et al., 2010) (Figure 8). Water from precipitation causes the infiltration and downward mixing of fresh precipitation with older equilibrated waters held in the unsaturated soils. The increased infiltration causes the water table to rise into the highly permeable zones at the base of the unsaturated soil zones. This, in turn, creates a condition of near lateral sub-surface flow of mixed waters from the unsaturated towards the small rivulets and streams throughout the watershed. This flow is commonly referred to as “interlayer” flow that comprises the bulk of the water recharging streams and wetlands throughout the watershed during periods of high to moderate flow (e.g., during our wet and early dry periods).

For mercury and DOC, the most important processes are those that impact the chemistry of the waters just prior to emergence into the open flowing water. According to Bishop and others, the water emerging into streams effectively “samples” pore fluids from saturated soils in the riparian zone. This is where much DOC is generated and, correspondingly, where the Hg and Fe chemistry of water entering the streams is largely determined. During high flow periods, the water entering streams throughout the watershed sample recently saturated portions of riparian zones. During lower flow periods, water entering the streams does so through deeply reacted, more permanently saturated reduced zones.

The model depicted in Figure 8 accounts for many of the geochemical trends shown in Figures 5 and 6. Initially, during the high flow period, interlayer flow throughout the watershed intersects recently unsaturated soils and the conditions are more oxidizing, taking place over shorter time periods, resulting in less Fe mobilization. Linear relationships between Fe and DOC during the early dry period indicate the flow paths deepen and become sufficiently reducing to mobilize high Fe. High Mg concentrations in background waters (e.g., the upward shift in Mg concentration) during this period are also consistent with greater reaction between the waters and minerals in the riparian sediments. Sulfate concentrations, however, decline to less than 1 mg/L (at Mile 179), as Fe begins to peak, indicating that SO₄ has generally been consumed along the flow path and so is no longer an important factor in geochemical reactions. However, since a similar amount of SO₄ will be reduced during recharge along the flow paths in virtually all of the non-mining portions of the watershed, it is reasonable to expect that the majority of MeHg generation and transport occurs in wetlands and riparian zones throughout the watershed.

SO₄ introduced through mining, is not recharged through the soils in riparian zones, at least not in the same way as SO₄ delivered throughout the watershed by precipitation or generated by the weathering of minerals in soils. There is likely to be some intersection of SO₄ derived from mining with saturated soils in wetlands or in reduced sediments and waters from lake bottoms,

but the data collected in this and other related studies (Bailey et al 2014 a,b. Johnson et al., 2014) suggest these reactions are not, by comparison, important MeHg sources compared to the natural background sources owing to ineffective transport. SO₄ delivered to the watershed through precipitation, meanwhile, is directed entirely into riparian zone soils and the resultant MeHg that is generated is directed into the streams as part of the natural interlayer flow that accompanies stream recharge following rain events.

Summary and Implications

Thirty-three samples collected upstream and downstream from the mining region during a summer that included both wet and dry extremes revealed no statistical relationship between SO₄ and MeHg concentration in the river. Thus, using a purely statistical approach it would seem that simply changing the amount of SO₄ delivered from the mining region would have negligible effect on MeHg concentrations in the river. While there is widespread acceptance that SO₄ reduction is a primary process responsible for generation and production of MeHg in natural waters, the data collected in this study suggest that MeHg found in the St. Louis River is produced by processes occurring during SO₄ reduction associated with recharge in non-mining areas and that SO₄ pumped from mines is essentially disconnected from that process. Strong linear correlation between Mg and SO₄, two major components in mine waters, support this interpretation.

Seasonal MeHg, THg, Fe, and DOC concentrations upstream and downstream from the region can be accounted for by a model involving the sequential reduction of SO₄ and Fe along the flow paths for waters recharging streams in riparian zones and wetlands. While SO₄ concentration in waters from non-mining areas is much lower than in mining areas, its reduction to sulfide is almost certain to occur when it is transported through organic rich soils as rivers are recharged. This contrasts sharply to the behavior of SO₄ pumped directly into rivers from mines which largely avoids SO₄ reduction and related Hg methylation, even during and following periods of high flow.

The St. Louis River is one of many rivers and lakes throughout the state that has fish Hg concentrations above acceptable limits, but this is the only watershed with such a strong mining-SO₄ component. While SO₄ from mining is often considered to play an important role in the generation and delivery of MeHg to the St. Louis River, the results of this study do not support that interpretation. The indiscriminate controlling of SO₄ discharges from mines would likely prove to be an ineffective strategy for decreasing MeHg concentrations in St. Louis River waters.

A parallel study, evaluated relationships between MeHg concentration in water and in dragonfly larvae (Jeremiason et al., 2014a) to determine whether some other factor related to mining (e.g., high ionic strength or DOC quality or quantity) were primary factors impacting bioaccumulation of MeHg at the lower trophic levels. While this latter study was not conclusive, it revealed strong correlations between averaged MeHg in the water column and MeHg in the larvae collected in the fall of 2012. This finding, used in conjunction with data from the present study imply that controlling MeHg by controlling SO₄ introduced from the mining industry would likely prove to be ineffective at controlling MeHg concentrations not just in water, but also in the local biota.

The Minnesota Pollution Control Agency is conducting additional studies that began in 2013 to test hypothesis generated in the present study and also to determine impacts of SO₄ to MeHg bioaccumulation in the St. Louis River estuary, where MeHg concentrations in fish are elevated well above those in the St. Louis River covered by the present studies.

Acknowledgements

This work was a funded by the DNR's Environmental Cooperative Research and Iron Ore Cooperative Research Program as well as by Minnesota's Environmental and Natural Resources Trust Fund. We thank Edward Swain and Bruce Monson from MPCA, Megan Kelly from the DNR, Nathan Johnson from the University of Minnesota Duluth, Daniel Engstrom from the Minnesota Science Museum, and Carl Mitchell from the University of Toronto for numerous useful discussions as this research project was developed and conducted. We also thank George Aiken and Kenna Butler for conducting SUVA and DOC analyses of the samples and providing constructive criticism relating to transport of DOC.

Figures

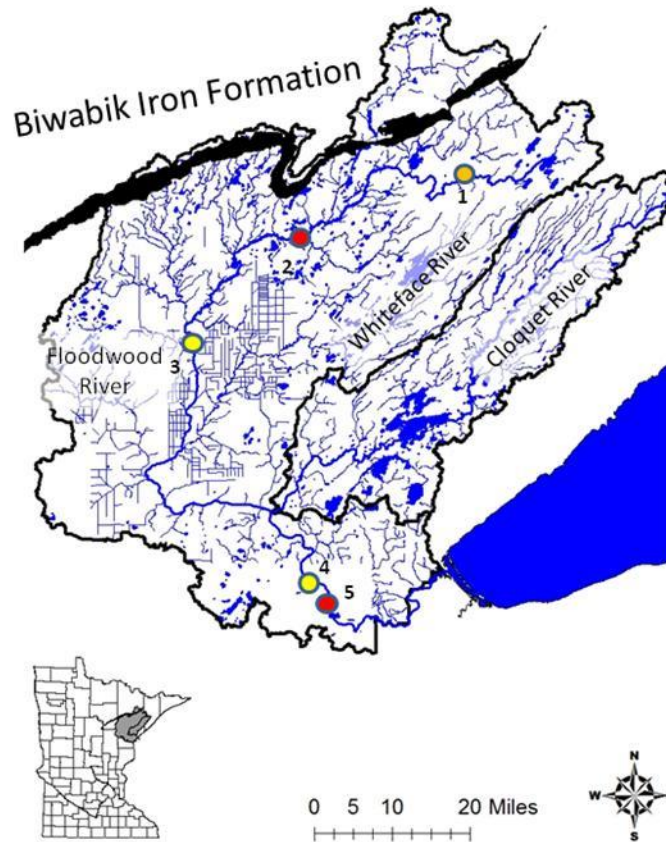


Figure 1. Location map showing the St. Louis River watershed in relation to the Biwabik Iron formation and five study sites. (1) Skibo/Mile 179 (Chemistry and flow upstream from mining influence), (2) Forbes (flow only), (3) Mile 94 (Chemistry following input from the last mining tributary), (4) Mile 36 (chemistry following dilution of mining inputs from many non-mining tributaries, including Whiteface, Floodwood, and Cloquet Rivers, (5) Scanlon, flow only. See Table 1 for site descriptions.

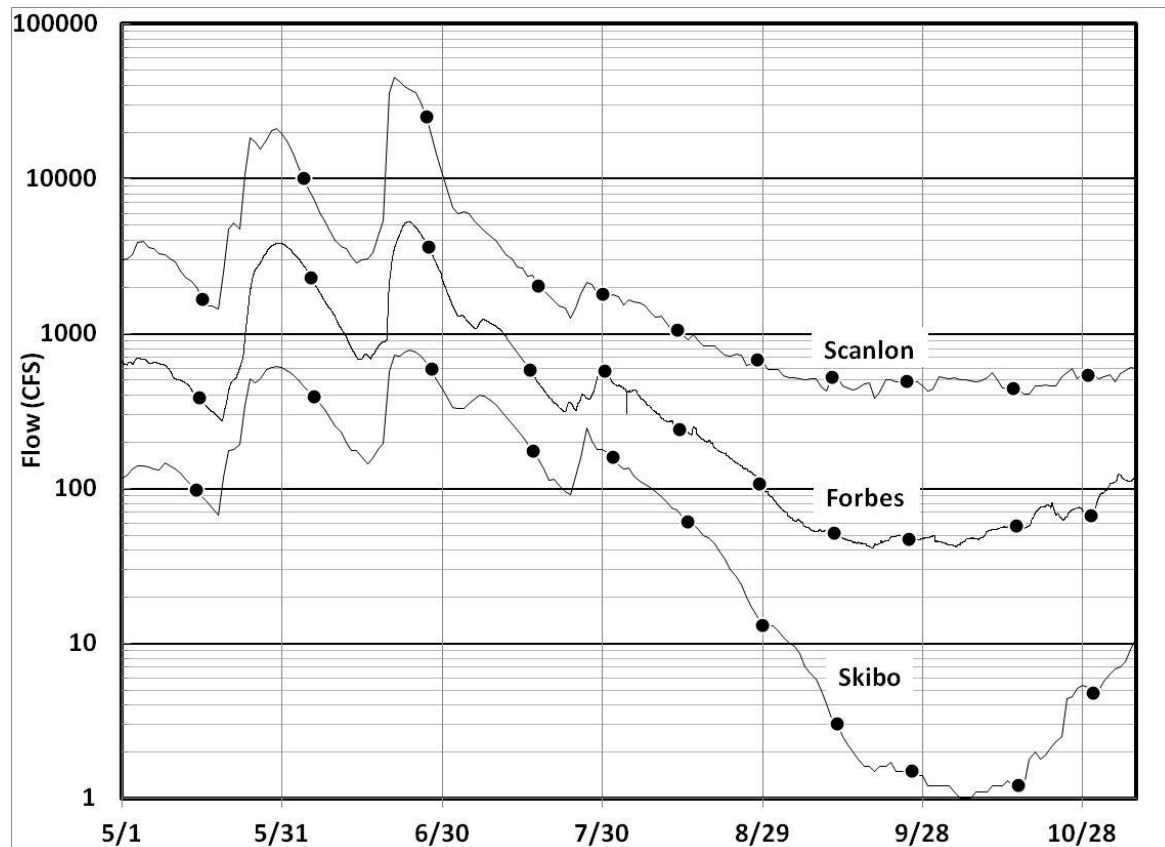


Figure 2. Flow versus time for three stations in the St. Louis River. Black circles represent dates when samples were collected at the site or from other sites nearby. Hydrographs were very similar for all three sites suggesting that the hydrologic conditions changed relatively systematically throughout the watershed from generally wet, fueled by large and widespread rain events in May and June, but generally dry conditions July through October.

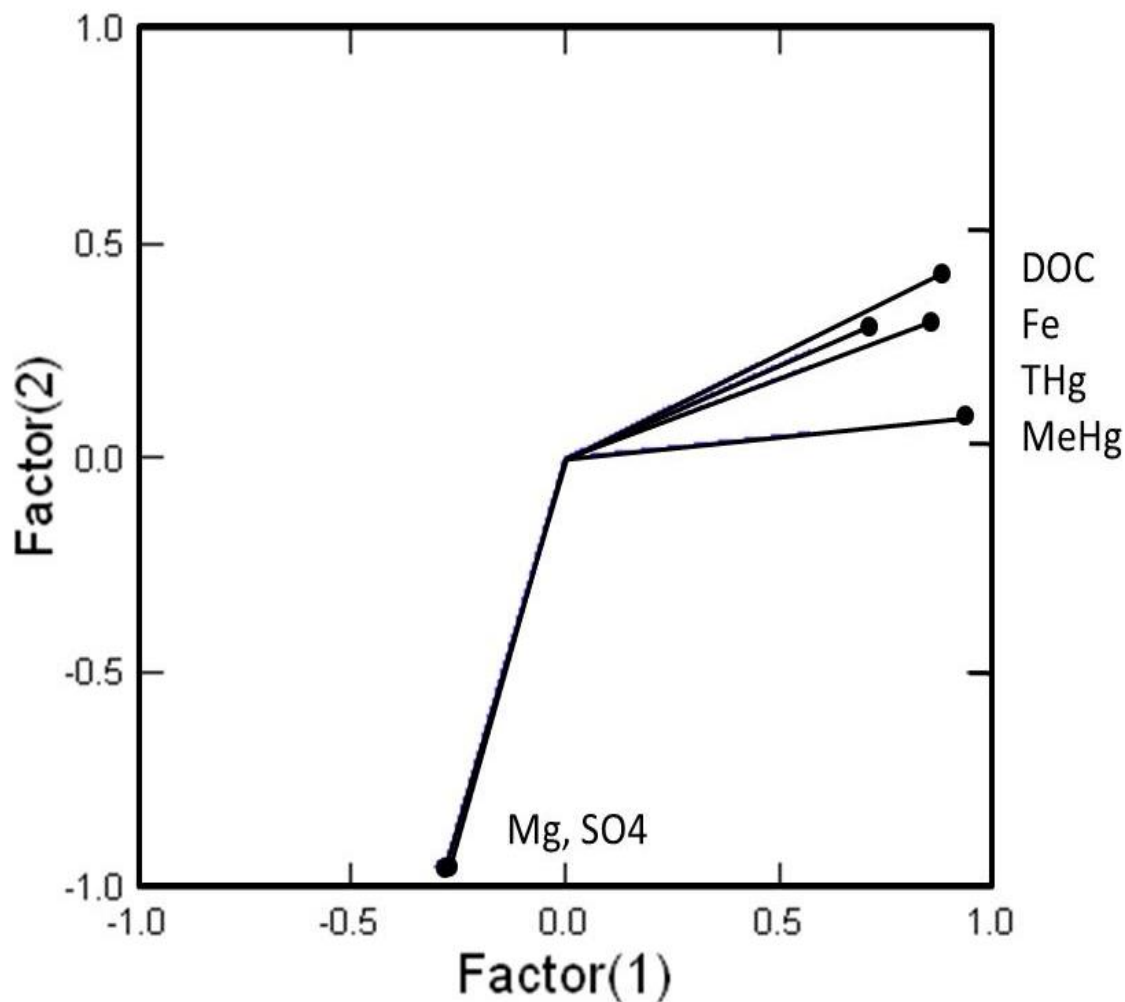


Figure 3. Factor loadings plot from a principal component analyses performed on the DOC, Fe, THg, MeHg, Mg, and SO₄ for the 33 samples collected during the present study. Parameters that are related to each other plot in the same general area, while those unrelated to each other plot orthogonally to each other. Mg and SO₄, which in this watershed are derived principally from the mining region, plot orthogonal to DOC, Fe, THg, and MeHg, which are derived principally from the non-mining region. MeHg and SO₄ concentrations are almost unrelated to each other in the St. Louis River, but a slightly negative correlation is exhibited between SO₄ and DOC, Fe, and THg.

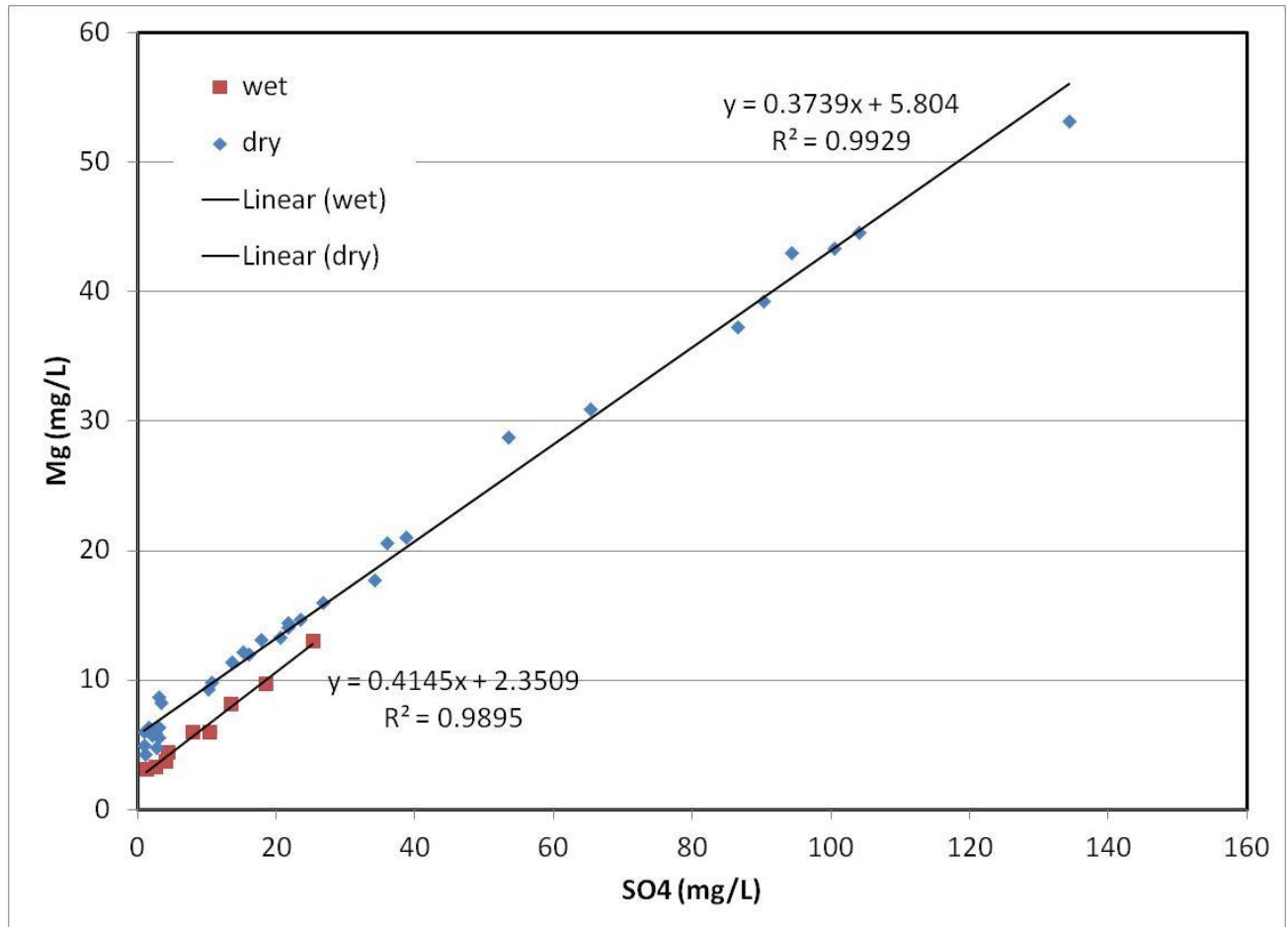


Figure 4. Mg vs SO4 for the 33 samples collected during the present study. “Wet” refers to samples collected in May and June, when frequent rains caused conditions to reach very high flow levels throughout the watershed. “Dry” refers to samples collected during the remainder of the summer when the watershed received very little rain. Two parallel mixing trends developed indicating that water from the mines with high Mg and SO4 was simply mixing without much reaction into a watershed with low but shifting Mg and SO4 concentrations.

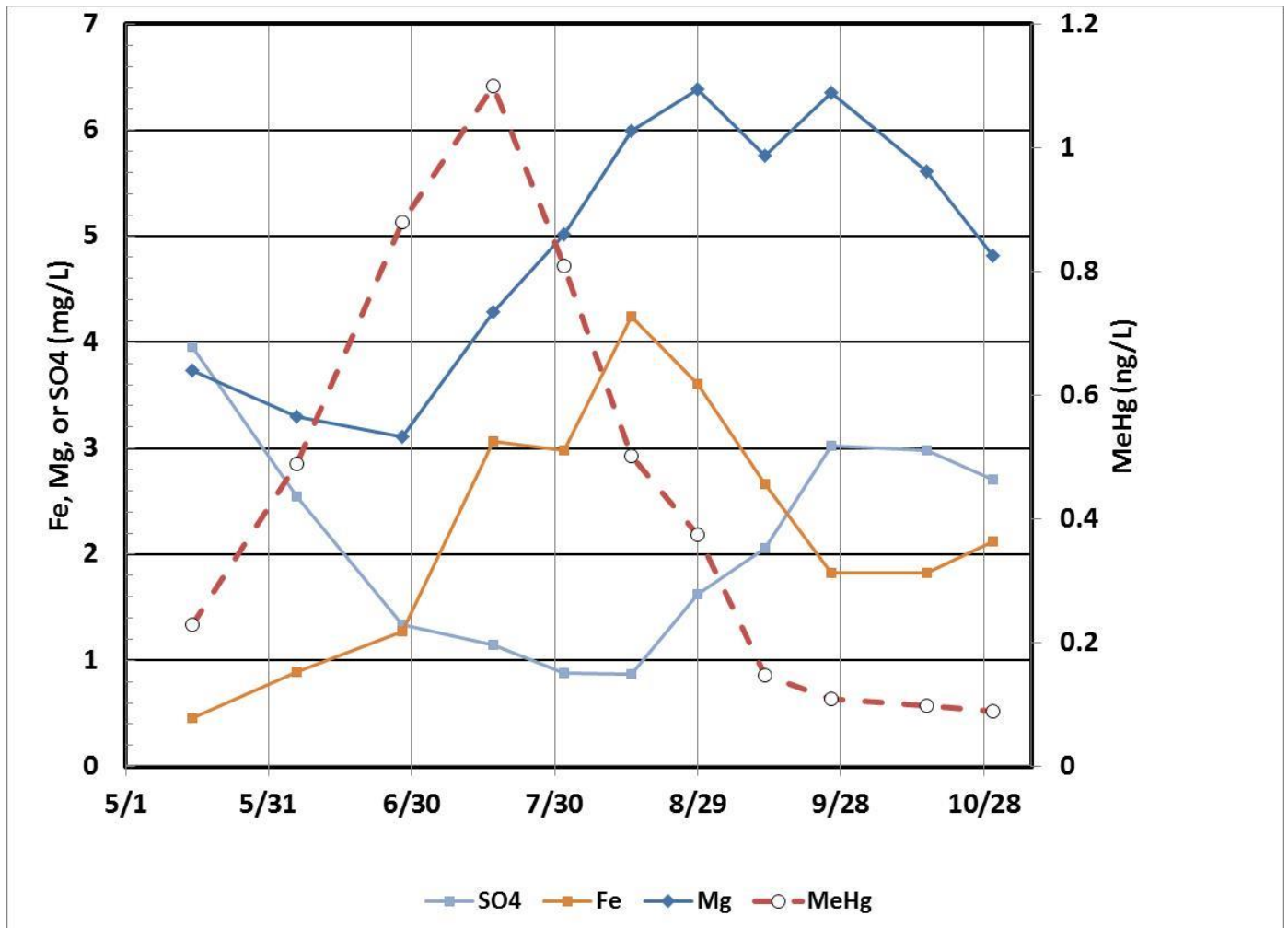


Figure 5. SO₄, Fe, Mg, and MeHg concentrations as a function of time for Mile 179, upstream from the mining region. Here, Mg and SO₄ were anti-correlated, with SO₄ concentrations decreasing eventually to < 1 mg/L during the wet and early dry period as Mg increased eventually up to around 6 mg/L. Similar chemical processes throughout the watershed explain the shift in Mg vs. SO₄ trends that occurred as wet conditions transition to dry in Figure 4. MeHg concentrations peaked as SO₄ approached 1 mg/L but then declined thereafter. Fe concentrations were elevated throughout indicating that that redox conditions were sufficiently reducing to promote conversion of SO₄ to sulfide during this time.

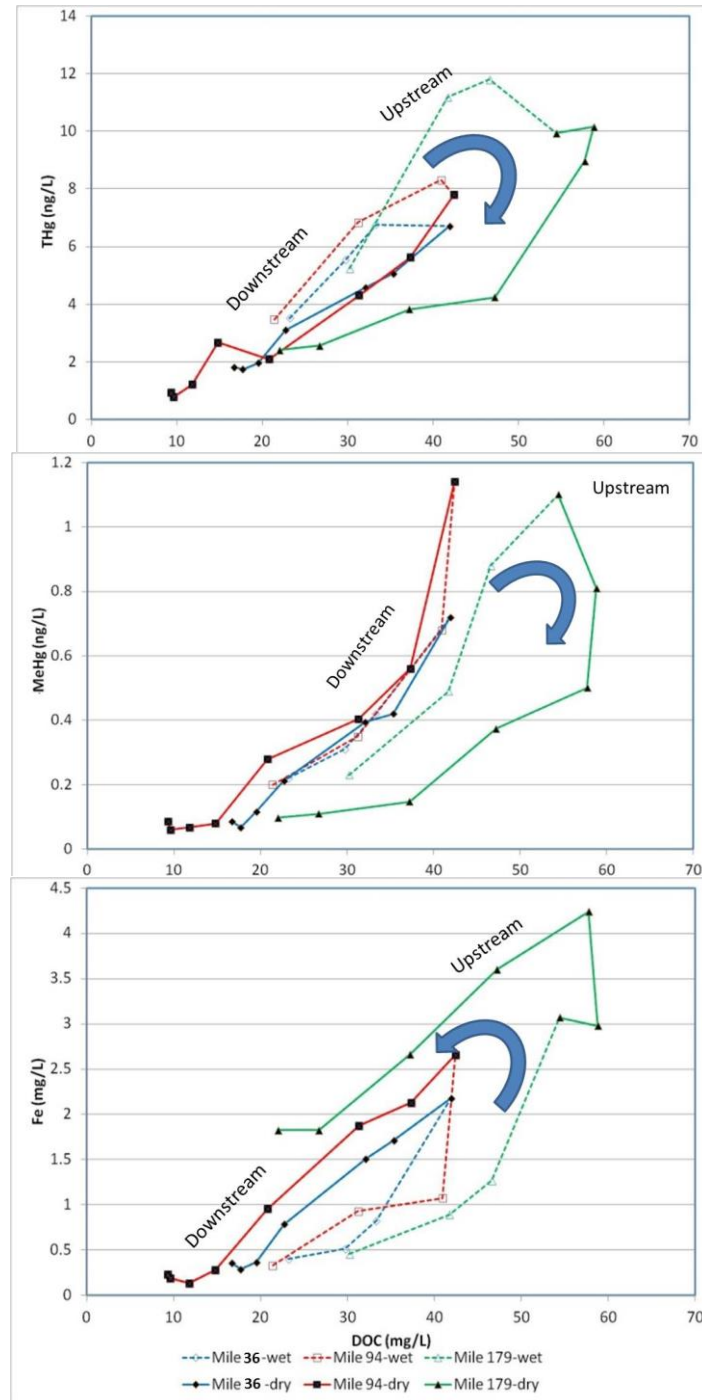


Figure 6. THg, MeHg and Fe concentrations as functions of DOC both upstream (Mile 36) and downstream (Mile 179) from the mining region. Conditions switched from wet (dashed) to dry (solid) and created distinct changes in the transport of MeHg, THg, Fe, and DOC. The upstream site appeared to carry an additional DOC component with lower THg and very little MeHg during the dry period. However, higher Fe and parallel Fe-DOC mixing trends suggests a deepening of recharge flow paths occurred throughout the watershed during this period.

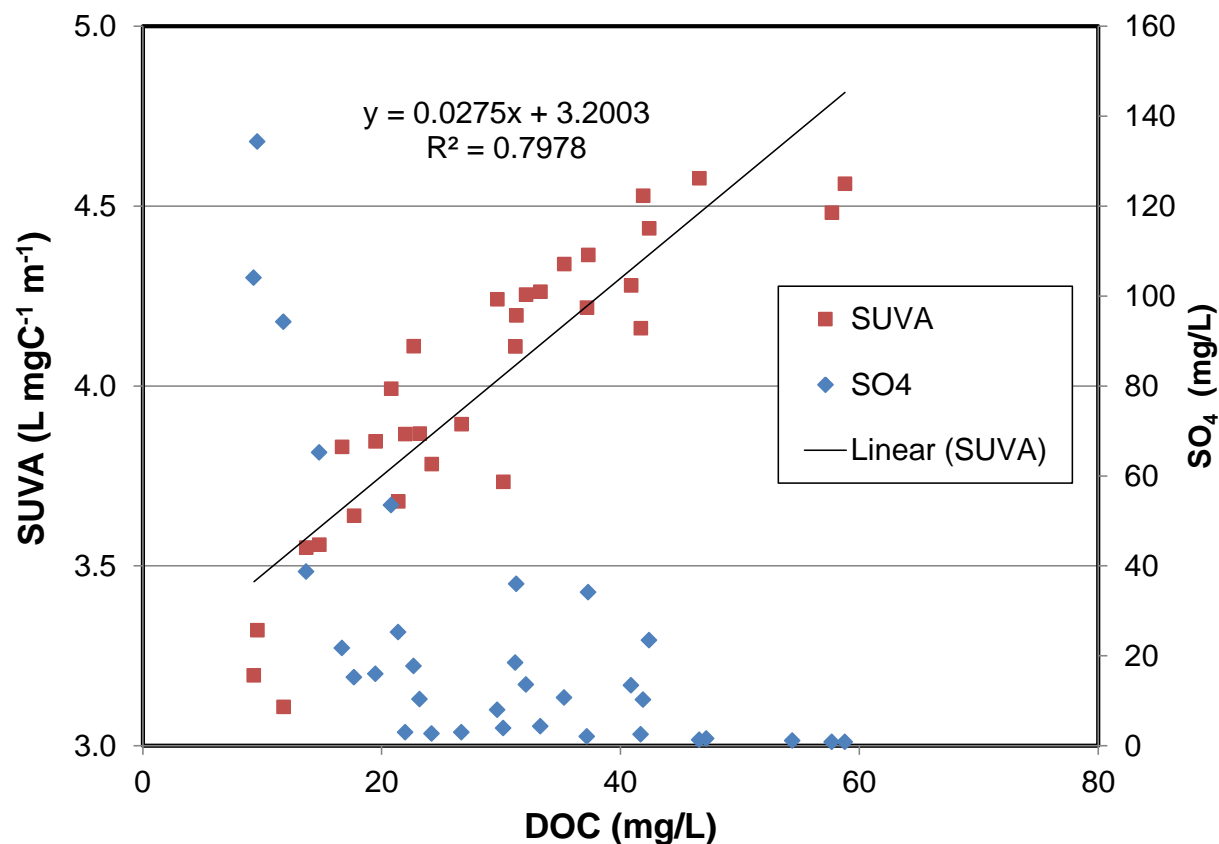


Figure 7: Fe-corrected SUVA and dissolved SO₄ concentration as a function of DOC concentration. Waters with elevated SO₄ carry generally less DOC with lower SUVA values than waters with low SO₄ concentration. This suggests that addition of components from mining (SO₄, Mg, Ca, alkalinity) may limit the mobility of high-SUVA DOC.

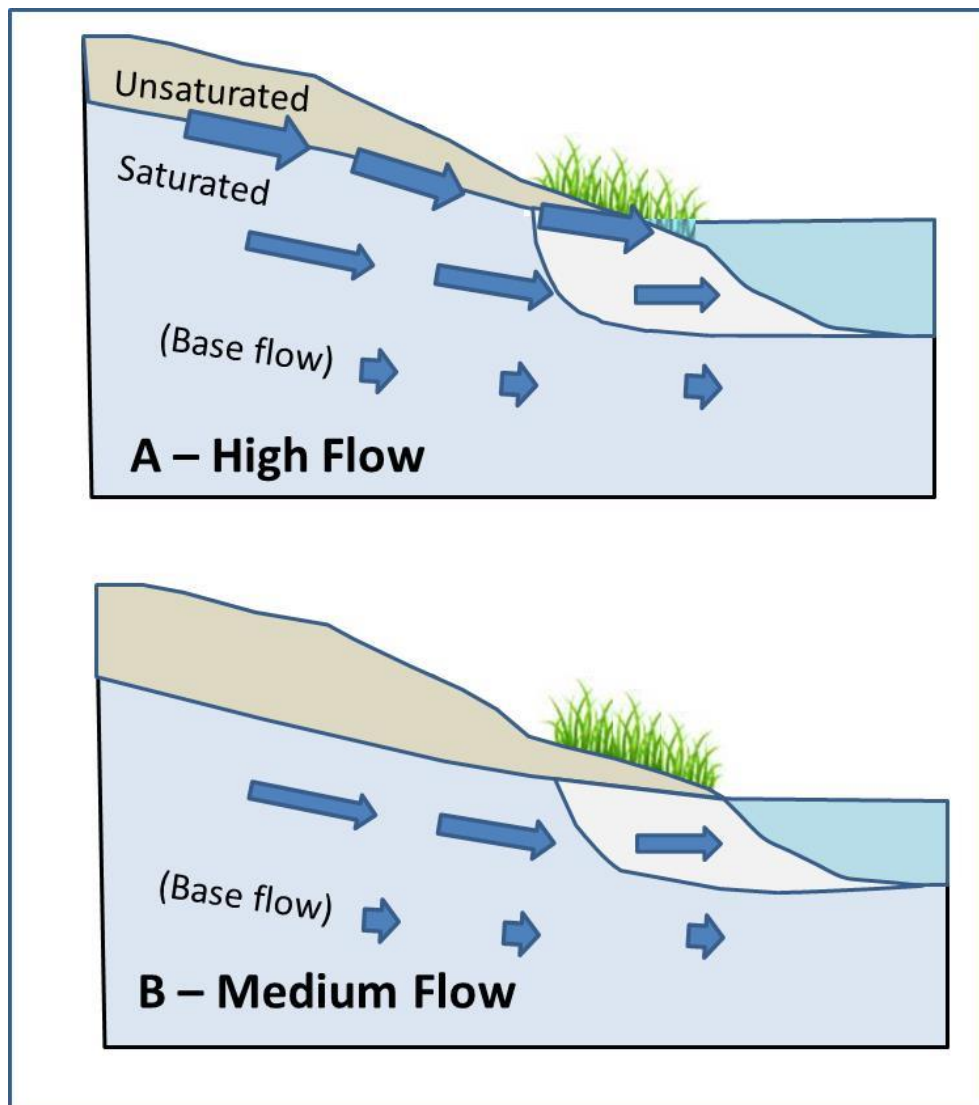


Figure 8: Schematic representation of how DOC, MeHg, THg, and Fe concentrations become elevated in the St. Louis River watershed. Water containing small amounts of SO_4 from groundwater or weathered from soils is pushed into and through organic rich sediments in riparian zones and wetlands (light-shaded zone). Biologic reactions deplete the SO_4 and produce DOC, MeHg, THg, and Fe along the flow path. Under wet, high flow conditions (A) a majority of the water enters streams through shallow, more oxidized flow paths and have less Fe and slightly different MeHg/DOC and THg/DOC ratios than water entering the stream under reduced flow conditions (B). Under extreme low-flow “base flow” conditions, water is dominated by direct groundwater recharge (e.g., springs) which has low DOC and may not interact with organic carbon along its flow path.

Tables

Table 1. Location Descriptions. River miles is the approximated distance upstream from the Estuary on Lake Superior.

River Mile	Location	Gaging	Chemistry?
33 - Scanlon	Scanlon Dam	USGS #04024000	No
36	Highway 33 Bridge		Yes
94	Highway 52 Bridge		Yes
125	United Taconite Access Road	DNR #03115001	No
179 - Skibo	110 Bridge E of Hoyt Lakes	USGS #04015438	Yes

Table 2. Measured flow and concentrations for selected dissolved compounds for miles 36, 94, and 179.

Date	Flow (cfs)	DOC mg/L	THg ng/L	MeHg ng/L	Fe mg/L	SO4 mg/L	Mg mg/L	Ca mg/L
Mile 36								
05/16/12	2000	23.2	3.5	0.22	0.40	10.4	6.0	15.0
06/04/12	8560	29.7	5.5	0.31	0.52	8.0	6.0	11.6
06/27/12	25200	33.3	6.8	0.42	0.83	4.4	4.4	10.5
07/18/12	2350	41.9	6.7	0.72	2.18	10.3	9.3	16.3
07/30/12	1800	35.3	5.1	0.42	1.71	10.7	9.8	17.1
08/13/12	1050	32.1	4.6	0.39	1.51	13.6	11.4	17.9
08/28/12	676	22.7	3.1	0.21	0.79	17.7	13.1	19.3
09/11/12	518	19.5	2.0	0.12	0.37	16.0	12.0	17.9
09/25/12	488	17.7	1.7	0.07	0.29	15.2	12.2	19.1
10/15/12	441	16.7	1.8	0.09	0.35	21.7	14.4	20.5
10/29/12	539	13.7	1.4	0.07	0.36	38.7	21.1	25.2
Mile 94								
05/15/12	672	21.4	3.5	0.20	0.33	25.3	13.0	17.4
06/05/12	4022	31.2	6.8	0.35	0.93	18.5	9.8	13.6
06/27/12	6313	40.9	8.3	0.68	1.07	13.4	8.2	12.5
07/16/12	1012	42.4	7.8	1.14	2.66	23.5	14.7	17.2
07/30/12	996	37.3	5.6	0.56	2.13	34.1	17.8	18.1
08/13/12	419	31.3	4.3	0.40	1.87	36.0	20.6	20.8
08/28/12	188	20.8	2.1	0.28	0.95	53	28.8	26.0
09/11/12	90	14.8	2.7	0.08	0.28	65	31.0	27.6
09/25/12	82	11.8	1.2	0.07	0.14	94	43.1	33.4
10/15/12	100	9.6	0.8	0.06	0.19	134	53.2	37.9
10/29/12	117	9.3	0.9	0.09	0.23	104	44.6	36.7
Mile 179								
05/15/12	97	30.2	5.2	0.23	0.46	3.95	3.7	5.1
06/06/12	391	41.7	11.2	0.49	0.89	2.55	3.3	5.0
06/28/12	586	46.6	11.8	0.88	1.27	1.34	3.1	5.5
07/17/12	174	54.4	9.9	1.10	3.07	1.14	4.3	7.0
08/01/12	158	58.8	10.2	0.81	2.98	0.88	5.0	7.7
08/15/12	61	57.7	9.0	0.50	4.24	0.88	6.0	8.5
08/29/12	13	47.2	4.2	0.37	3.60	1.62	6.4	8.6
09/12/12	3.0	37.2	3.8	0.15	2.66	2.06	5.8	8.1
09/26/12	1.5	26.7	2.6	0.11	1.82	3.02	6.4	8.9
10/16/12	1.2	22.0	2.4	0.10	1.83	2.99	5.6	8.1
10/30/12	4.8	24.2	2.3	0.09	2.12	2.70	4.8	6.3

Appendix - Data Tables

Table A-1. Physical and chemical parameters measured at SLR 36. Unless otherwise specified, concentrations are in mg/L.

Date	5/16	6/4	6/27	7/18	7/30	8/13	8/28	9/11	9/25	10/15	10/29
Time	8:52	11:54	9:11	9:41	13:18	11:47	12:21	13:31	11:51	14:13	11:03
Flow (cfs)	2,000	8,560	25,200	2,350	1,800	1,050	676	518	488	441	539
pH	7.6	7.1	6.9	7.5	7.4	7.0	7.9	7.9	8.1	8.4	6.3
Spec. Cond. (µS/cm)	167	115	90	153	175	197	218	223	210	241	315
Temp (°C)	16.9	17.1	19.6	24.4	25.6	22.3	23.6	18.4	12.9	7.2	5.2
Dissolved Oxygen	9.6	7.6	5.9	5.5	6.5	6.5	7.7	7.9	10.2	13.2	13.5
ORP (mv)	87	64	119	233	100	135	150	88	-72	111	153
SUVA (L/mg C/m)	3.9	4.2	4.3	4.5	4.3	4.3	4.1	3.8	3.6	3.8	3.6
DOC	23.2	29.7	33.3	41.9	35.3	32.1	22.7	19.5	17.7	16.7	13.7
F-MeHg (ng/L)	0.22	0.31	0.42	0.72	0.42	0.39	0.21	0.12	0.07	0.09	0.07
F-THg (ng/L)	3.5	5.5	6.8	6.7	5.1	4.6	3.1	2.0	1.7	1.8	1.4
Al	0.05	0.12	0.16	0.11	0.09	0.06	0.03	0.02	0.02	0.03	0.02
Ba	0.01	0.06	0.10	0.03	0.07	0.02	0.02	0.03	0.03	0.02	0.02
Ca	15.0	11.6	10.5	16.3	17.1	17.9	19.3	17.9	19.1	20.5	25.2
Fe	0.40	0.52	0.83	2.2	1.7	1.5	0.79	0.37	0.29	0.35	0.36
K	0.932	0.855	0.927	1.28	1.33	1.29	1.39	1.31	1.31	1.50	1.91
Mg	5.98	5.98	4.43	9.32	9.81	11.4	13.1	12.0	12.2	14.4	21.1
Mn	0.088	0.067	0.063	0.117	0.090	0.065	0.010	0.008	0.011	0.032	0.041
Na	5.17	3.52	2.64	5.04	5.11	5.98	6.69	6.19	6.30	7.27	9.95
P	0.011	0.020	0.027	0.040	0.039	0.025	0.015	-0.007	0.002	0.010	0.009
Si	1.8	2.8	3.1	4.5	4.9	4.9	4.1	3.1	3.6	4.1	4.0
Sr	0.043	0.039	0.033	0.049	0.051	0.056	0.061	0.056	0.059	0.061	0.074
Fluoride	0.076	0.076	0.067	0.088	0.113	0.139	0.135	0.122	0.121	0.142	0.140
Acetate	< 0.01	< 0.01	< 0.01	< 0.01	< 0.01	< 0.01	< 0.01	< 0.01	< 0.01	< 0.01	< 0.01
Formate	< 0.01	< 0.01	< 0.01	< 0.01	< 0.01	< 0.01	< 0.01	< 0.01	< 0.01	< 0.01	< 0.01
Chloride	5.16	2.68	1.69	3.96	4.60	4.78	5.50	5.65	5.60	6.39	9.69
Bromide	< 0.006	< 0.006	< 0.005	0.008	0.011	0.009	0.008	< 0.005	< 0.005	< 0.005	0.005
Nitrate-N	1.04	0.075	0.057	0.219	0.539	0.212	0.047	< 0.001	0.025	-0.001	0.041
Sulfate	10.4	7.96	4.36	10.3	10.7	13.6	17.7	16.0	15.2	21.7	38.7
Oxalate	< 0.01	< 0.01	< 0.01	< 0.01	< 0.01	< 0.01	< 0.01	< 0.01	< 0.01	< 0.01	< 0.01
Thiosulfate	< 0.01	< 0.01	< 0.01	< 0.01	< 0.01	< 0.01	< 0.01	< 0.01	< 0.01	< 0.01	< 0.01
Phosphate-P	< 0.006	0.210	< 0.005	< 0.005	< 0.005	< 0.005	< 0.005	< 0.005	< 0.005	< 0.005	< 0.005
Alkalinity	55	35	18	50	63	55	78	80	80	90	105
Ammonia-N	0.025	0.040	0.042	0.068	0.041	0.043	0.022	0.026	< 0.020	< 0.020	< 0.020
Nitrate/Nitrite	< 0.4	< 0.4	< 0.4	< 0.4	< 0.4	< 0.4	< 0.4	< 0.4	< 0.4	< 0.4	< 0.4
TKN	0.91	1.2	1.4	1.4	1.3	1.1	0.84	0.64	0.68	0.71	< 0.50
Total P	0.04	0.08	0.09	0.08	0.06	0.05	0.03	0.02	0.02	0.02	0.02

Table A-2. Physical and chemical parameters measured at SLR 94. Flow was measured at SLR Mile 132. Unless otherwise specified, concentrations are in mg/L.

	5/15	6/5	6/27	7/16	7/30	8/13	8/28	9/11	9/25	10/15	10/29
Time	13:22	12:24	11:18	11:13	11:30	10:10	10:22	12:02	10:28	12:58	13:08
Flow (cfs)	672	4,022	6,313	1,012	996	419	188	90	82	100	117
pH	7.9	7.3	7.1	7.5	7.8	7.9	8.1	8.3	8.3	8.4	7.7
Spec. Cond. (µS/cm)	254	168	140	221	262	282	412	503	581	673	582
Temp (°C)	17.4	18.1	20.3	24.7	23.8	20.9	20.1	16.9	9.2	6.6	4.4
Dissolved Oxygen	9.9	8.1	6.8	6.4	7.3	8.8	8.2	11.3	12.3	15.7	15.6
ORP (mv)	186	145	124	133	92	121	141	52	-41	137	127
SUVA (L/mg C/m)	3.7	4.1	4.3	4.4	4.4	4.2	4.0	3.6	3.1	3.3	3.2
DOC	21.4	31.2	40.9	42.4	37.3	31.3	20.8	14.8	11.8	9.6	9.3
F-MeHg (ng/L)	0.20	0.35	0.68	1.14	0.56	0.40	0.28	0.08	0.07	0.06	0.09
F-THg (ng/L)	3.5	6.8	8.3	7.8	5.6	4.3	2.1	2.7	1.2	0.8	0.9
Al	0.04	0.31	0.18	0.14	0.10	0.07	0.04	0.01	0.01	0.01	0.01
Ba	0.02	0.07	0.05	0.04	0.02	0.03	0.02	0.04	0.04	0.03	0.02
Ca	17.4	13.6	12.5	17.2	18.1	20.8	26.0	27.6	33.4	37.9	36.7
Fe	0.33	0.93	1.1	2.7	2.1	1.9	0.95	0.28	0.14	0.19	0.23
K	1.61	1.48	1.30	1.95	1.99	2.41	3.24	3.58	4.96	4.80	4.59
Mg	13.0	9.76	8.22	14.7	17.8	20.6	28.8	31.0	43.1	53.2	44.6
Mn	0.059	0.101	0.078	0.079	0.074	0.076	0.055	0.044	0.055	0.077	0.060
Na	8.39	6.02	4.87	8.32	9.07	11.2	16.0	19.2	23.0	22.9	21.6
P	0.010	0.025	0.025	0.040	0.032	0.029	0.018	< 0.004	0.005	0.007	0.006
Si	2.0	3.6	3.7	4.6	4.9	4.9	3.3	2.7	3.3	3.7	4.0
Sr	0.062	0.054	0.048	0.063	0.070	0.080	0.100	0.105	0.126	0.134	0.127
Fluoride	0.093	0.080	0.077	0.111	0.143	0.162	0.185	0.213	0.221	0.265	0.217
Acetate	< 0.01	< 0.01	< 0.01	< 0.01	< 0.01	< 0.01	< 0.01	< 0.01	< 0.01	< 0.01	< 0.01
Formate	< 0.01	< 0.01	< 0.01	< 0.01	< 0.01	< 0.01	< 0.01	< 0.01	< 0.01	< 0.01	< 0.01
Chloride	8.10	4.91	3.67	6.33	6.59	8.36	12.3	17.0	16.5	19.3	18.4
Nitrate-N	0.186	1.09	0.077	0.331	0.590	0.299	0.199	0.203	0.073	0.169	0.274
Sulfate	25.3	18.5	13.4	23.5	34.1	36.0	53.5	65.2	94.3	134	104
Oxalate	< 0.01	< 0.01	< 0.01	< 0.01	< 0.01	< 0.01	< 0.01	< 0.01	< 0.01	< 0.01	< 0.01
Thiosulfate	< 0.01	< 0.01	< 0.01	< 0.01	< 0.01	< 0.01	< 0.01	< 0.01	< 0.01	< 0.01	< 0.01
Alkalinity	65	45	45	73	75	98	135	160	188	190	175
Ammonia-N	0.024	0.042	0.045	0.061	0.040	0.044	< 0.020	0.025	< 0.020	< 0.020	0.022
Nitrate/Nitrite	< 0.4	< 0.4	< 0.4	< 0.4	< 0.4	< 0.4	< 0.4	< 0.4	< 0.4	< 0.4	< 0.4
TKN	0.89	1.2	1.5	1.5	1.4	1.1	0.70	0.56	0.58	0.52	< 0.5
Total P	0.04	0.07	0.11	0.09	0.07	0.04	0.03	0.04	0.02	0.01	0.02

Table A-3. Physical and chemical parameters measured at SLR 179. Unless otherwise specified, concentrations are in mg/L.

Date	5/15	6/6	6/28	7/17	8/1	8/15	8/29	9/12	9/26	10/16	10/30
Time	8:32	8:47	9:28	8:51	11:55	11:02	10:47	10:54	10:27	9:10	12:47
Flow (cfs)	97	391	586	174	158	61	13	3.0	1.5	1.2	4.8
pH	7.1	6.4	6.5	6.9	6.7	7.1	7.2	7.4	7.8	8.0	8.7
Spec. Cond. (µS/cm)	55	46	42	54	63	63	74	89	94	92	72
Temp (°C)	16.3	18.6	22.0	25.5	23.8	19.6	19.2	15.3	6.4	5.9	1.9
Dissolved Oxygen	9.5	8.8	7.5	6.8	7.5	8.3	8.0	8.7	10.8	12.6	14.4
ORP (mv)	180	189	149	152	89	102	83	82	-48	155	95
SUVA (L/mg C/m)	3.7	4.2	4.6		4.6	4.5		4.2	3.9	3.9	3.8
DOC	30.2	41.7	46.6	54.4	58.8	57.7	47.2	37.2	26.7	22	24.2
F-MeHg (ng/L)	0.23	0.49	0.88	1.10	0.81	0.50	0.37	0.15	0.11	0.10	0.09
F-THg (ng/L)	5.2	11	12	9.9	10	9.0	4.2	3.8	2.6	2.4	2.3
Al	0.12	0.27	0.31	0.36	0.30	0.27	0.23	0.17	0.12	0.11	0.12
Ba	0.01	0.09	0.05	0.06	0.05	0.03	0.02	0.05	0.03	0.02	0.02
Ca	5.15	4.99	5.51	6.95	7.70	8.52	8.55	8.06	8.95	8.15	6.27
Fe	0.46	0.89	1.3	3.1	3.0	4.2	3.6	2.7	1.8	1.8	2.1
K	0.203	0.338	0.360	0.510	0.448	0.566	0.605	0.528	0.586	0.543	0.449
Mg	3.73	3.30	3.11	4.28	5.02	6.00	6.39	5.76	6.36	5.61	4.82
Mn	0.018	0.062	0.105	0.189	0.125	0.095	0.088	0.083	0.062	0.043	0.032
Na	1.88	1.51	1.44	1.57	1.37	1.51	1.94	1.85	2.41	2.33	2.30
P	0.005	0.010	0.015	0.028	0.024	0.021	0.032	0.022	0.016	0.022	0.023
Si	0.3	1.7	2.2	3.5	4.5	5.2	5.1	4.4	5.6	5.5	4.1
Sr	0.018	0.023	0.024	0.026	0.031	0.032	0.033	0.028	0.030	0.027	0.021
Fluoride	0.042	0.047	0.057	0.077	0.080	0.076	0.081	0.070	0.058	0.081	0.062
Acetate	< 0.01	< 0.01	< 0.01	< 0.01	< 0.01	< 0.01	< 0.01	< 0.01	< 0.01	< 0.01	< 0.01
Formate	< 0.01	< 0.01	< 0.01	< 0.01	< 0.01	< 0.01	< 0.01	< 0.01	< 0.01	< 0.01	< 0.01
Chloride	0.386	0.261	0.219	0.266	0.318	0.408	0.629	0.603	0.878	0.580	1.170
Nitrate-N	0.031	0.056	0.044	0.168	0.382	0.280	0.254	0.146	0.118	0.103	0.102
Sulfate	3.95	2.55	1.34	1.14	0.882	0.875	1.62	2.06	3.02	2.99	2.70
Oxalate	< 0.01	< 0.01	< 0.01	< 0.01	< 0.01	< 0.01	< 0.01	< 0.01	< 0.01	< 0.01	< 0.01
Thiosulfate	< 0.01	< 0.01	< 0.01	< 0.01	< 0.01	< 0.01	< 0.01	< 0.01	< 0.01	< 0.01	< 0.01
Phosphate-P	< 0.006	0.009	< 0.005	< 0.005	< 0.005	< 0.005	< 0.005	< 0.005	< 0.005	< 0.005	< 0.005
Alkalinity	15	13	15	18	20	25	25	35	40	40	25
Ammonia-N	0.025	0.058	0.060	0.147	0.095	0.062	0.033	0.042	0.041	0.022	0.023
Nitrate/Nitrite	< 0.4	< 0.4	< 0.4	< 0.4	< 0.4	< 0.4	< 0.4	< 0.4	< 0.4	< 0.4	< 0.4
TKN	1.08	1.4	1.6	1.8	1.9	1.7	1.5	1.1	0.89	0.77	0.76
Total P	0.02	0.04	0.04	0.05	0.05	0.05	0.03	0.03	0.03	0.02	0.04

References

- Åkerblom, S., Bishop, K., Björn, E., Lambertsson, L., Eriksson, T., Nilsson, M.B., 2013. Significant interaction effects from sulfate deposition and climate on sulfur concentrations constitute major controls on methylmercury production in peatlands. *Geochimica et Cosmochimica Acta* 102, 1-11.
- Bailey, L., Johnson, N., Mitchell, C., Engstrom, D., Berndt, M., Coleman-Wasak, J., 2014a. Geochemical factors influencing methylmercury production and partitioning in sulfate impacted lake sediments, University of Minnesota Duluth Research Report, Duluth, MN, 63 p.
- Bailey, L., Johnson, N., Mitchell, C., Engstrom, D., Kelly, M., Berndt, M., 2014b. Seasonal and spatial variations in methylmercury in the water column of sulfate-impacted lakes, University of Minnesota Duluth Research Report, Duluth, MN, 64 p.
- Balogh, S.J., Nollet, Y.H., Swain, E.B., 2004. Redox chemistry in Minnesota streams during episodes of increased methylmercury discharge. *Environmental Science and Technology*, 38, 4921-4927.
- Balogh, S.J., Swain, E.B., Nollet, Y.H., 2006. Elevated methylmercury concentrations and loadings during flooding in Minnesota rivers. *Science of The Total Environment*, 368, 138-148.
- Benoit, J.M., Gilmour, C.C., Mason, R.P., Heyes, A., 1999. Sulfide Controls on Mercury Speciation and Bioavailability to Methylating Bacteria in Sediment Pore Waters. *Environmental Science & Technology*, 33, 951-957.
- Bergman, I., Bishop, K., Tu, Q., Frech, W., Åkerblom, S., Nilsson, M., 2012. The Influence of Sulphate Deposition on the Seasonal Variation of Peat Pore Water Methyl Hg in a Boreal Mire. *PLoS ONE* 7, e45547.
- Berndt, M.E., Bavin, T.K., 2009. Sulfate and mercury chemistry of the St. Louis River in Northeastern Minnesota: A Report to the Minerals Coordinating Committee. Minnesota Department of Natural Resources, Division of Lands and Minerals, St. Paul, MN, p. 83.
- Berndt, M.E., Bavin, T.K., 2011. Sulfur and Mercury Cycling in Five Wetlands and a Lake Receiving Sulfate from Taconite Mines in Northeastern Minnesota: A Report to Iron Ore Cooperative Research Program, Minnesota Department of Natural Resources, St. Paul, MN, 77 p.
- Berndt, M.E., Bavin, T.K., 2012a. On the cycling of sulfur and mercury in the St. Louis River watershed, Northeastern Minnesota. An Environmental and Natural Resources Trust Fund Final Report. St. Paul, MN, 91 p.

Berndt, M.E., Bavin, T.K., 2012b. Methylmercury and dissolved organic carbon relationships in a wetland-rich watershed impacted by elevated sulfate from mining. *Environmental Pollution*, 161, 321-327.

Bishop, K., Seibert, J., Köhler, S., Laudon, H., 2004. Resolving the Double Paradox of rapidly mobilized old water with highly variable responses in runoff chemistry. *Hydrological Processes*, 18, 185-189.

Brigham, M.E., Wentz, D.A., Aiken, G.R., Krabbenhoft, D.P., 2009. Mercury Cycling in Stream Ecosystems. 1. Water Column Chemistry and Transport. *Environmental Science & Technology*, 43, 2720-2725.

Burns, D.A., Aiken, G.R., Bradley, P.M., Journey, C.A., Schelker, J., 2013. Specific ultra-violet absorbance as an indicator of mercury sources in an Adirondack River basin. *Biogeochemistry*, 113, 451-466.

Coleman-Wasik, J., Mitchell, C.P.J., Engstrom, D.R., Swain, E.B., Monson, B.A., Balogh, S.J., Jeremiason, J.D., Branfireun, B.A., Eggert, S.L., Kolka, R.K., Almendinger, J.E., 2012. Methylmercury Declines in a Boreal Peatland When Experimental Sulfate Deposition Decreases. *Environmental Science & Technology*, 46, 6663-6671.

Corrales, J., Naja, G.M., Dziuba, C., Rivero, R.G., Orem, W., 2011. Sulfate threshold target to control methylmercury levels in wetland ecosystems. *Science of The Total Environment*, 409, 2156-2162.

Fitzgerald, W.F., Gill, G.A., 1979. Subnanogram determination of mercury by two-stage gold amalgamation and gas phase detection applied to atmospheric analysis. *Analytical Chemistry*, 51, 1714-1720.

Gerbig, C.A., Kim, C.S., Stegemeier, J.P., Ryan, J.N., Aiken, G.R., 2011. Formation of Nanocolloidal Metacinnabar in Mercury-DOM-Sulfide Systems. *Environmental Science & Technology*, 45, 9180-9187.

Gilmour, C., Riedel, G.S., Ederington, M.C., Bell, J.T., Gill, G.A., Stordal, M.C., 1998. Methylmercury concentrations and production rates across a trophic gradient in the northern Everglades. *Biogeochemistry*, 40, 327-345.

Gilmour, C.C., Henry, E.A., Mitchell, R., 1992. Sulfate stimulation of mercury methylation in freshwater sediments. *Environmental Science & Technology*, 26, 2281-2287.

Grabs, T., Bishop, K.H., Laudon, H., Lyon, S.W., Seibert, J., 2012. Riparian zone processes and soil water total organic carbon (TOC): Implications for spatial variability, upscaling and carbon exports. *Biogeosciences Discussions*, 9, 3031-3069.

Hintelmann, H., Evans, R.D., 1997. Application of stable isotopes in environmental tracer studies – Measurement of monomethylmercury (CH₃Hg⁺) by isotope dilution ICP-MS and detection of species transformation. *Fresenius J Anal Chem*, 358, 378-385.

Jeremiason, J., Reiser, K., Weitz, R., and Berndt, M., 2014a. Mercury in Dragonflies as Indicators of Methylmercury Contamination in Systems Receiving Elevated Sulfate Loading, Gustavus Adolphus College Research Report. St. Peter, MN, 24 p.

Jeremiason, J., Walker, M., Voigt, B., and Aiken, G. 2014b. Binding of MeHg to Dissolved Organic Matter. Gustavus Adolphus Research Report. St. Peter, MN, 23 p.

Jeremiason, J.D., Portner, J., Latch, D., and Aiken, G. 2014c. Methylmercury Photodegradation: Laboratory and Field Studies in the St. Louis River, Gustavus Adolphus College Research Report, St. Peter, MN, 23 p.

Jeremiason, J.D., Engstrom, D.R., Swain, E.B., Nater, E.A., Johnson, B.M., Almendinger, J.E., Monson, B.A., Kolka, R.K., 2006. Sulfate addition increases methylmercury production in an experimental wetland. *Environmental Science and Technology*, 40, 3800-3806.

Johnson, N., Mitchell, C., Engstrom, D., Bailey, L., Kelley, M., Berndt, M., 2014. Methyl mercury production and transport in a sulfate-impacted sub-boreal wetland, University of Minnesota Duluth Research Report. Duluth, MN, 55 p.

Kelly, M., and Berndt, M., 2014. An updated isotopic analysis of sulfate cycling and mixing processes in the St. Louis River Watershed, Minnesota Department of Natural Resources Research Report, St. Paul, MN, in preparation.

Knorr, K.H., 2013. DOC-dynamics in a small headwater catchment as driven by redox fluctuations and hydrological flow paths – are DOC exports mediated by iron reduction/oxidation cycles? *Biogeosciences*, 10, 891-904.

Köhler, S.J., Buffam, I., Seibert, J., Bishop, K.H., Laudon, H., 2009. Dynamics of stream water TOC concentrations in a boreal headwater catchment: Controlling factors and implications for climate scenarios. *Journal of Hydrology*, 373, 44-56.

Lyon, S.W., Grabs, T., Laudon, H., Bishop, K.H., Seibert, J., 2011. Variability of groundwater levels and total organic carbon in the riparian zone of a boreal catchment. *Journal of Geophysical Research G: Biogeosciences*, 116.

Maderak, M.L., 1963. Quality of waters, Minnesota, A compilation, 1955-1962. State of Minnesota Department of Conservation Division of Waters, St. Paul, MN.

Marvin-DiPasquale, M., Agee, J., McGowan, C., Oremland, R.S., Thomas, M., Krabbenhoft, D., Gilmour, C.C., 2000. Methyl-mercury degradation pathways: A comparison among three mercury-impacted ecosystems. *Environmental Science & Technology*, 34, 4908-4916.

Moyle, J.B., Kenyon, W.A., 1947. A biologic survey and fishery management plan for the streams of the Saint Louis River basin. Minnesota Department of Conservation.

MPCA, 2013. St. Louis River Monitoring and Assessment Report, in: Agency, M.P.C. (Ed.). Minnesota Pollution Control Agency, St. Paul, MN, 200 p.

Seibert, J., Grabs, T., Kohler, S., Laudon, H., Winterdahl, M., Bishop, K., 2009. Linking soil- and stream-water chemistry based on a Riparian Flow-Concentration Integration Model. *Hydrol. Earth Syst. Sci.*, 13, 2287-2297.

Vidon, P., Allan, C., Burns, D., Duval, T.P., Gurwick, N., Inamdar, S., Lowrance, R., Okay, J., Scott, D., Sebestyen, S., 2010. Hot Spots and Hot Moments in Riparian Zones: Potential for Improved Water Quality Management¹. *JAWRA Journal of the American Water Resources Association* 46, 278-298.